

# UV Pulsations in the Auroral Region According to Measurements on the Lomonosov Satellite



P. A. Klimov and K. F. Sigaeva

**Abstract** The Lomonosov satellite was launched into a  $97.3^\circ$  polar sun-synchronous orbit on April 26, 2016, and operated in orbit until December 2017. The TUS detector is a highly sensitive telescope, designed for both detection of ultra-high-energy cosmic rays and the Earth's atmosphere UV-radiation in the 240–400 nm range. To measure variety of atmospheric phenomena the telescope has four modes of operation with different temporal resolutions (from  $0.8 \mu\text{s}$  to 6.6 ms). Among the events recorded above  $50^\circ$  N in the mode with a temporal resolution of 6.6 ms, 66 were identified with an unusual spatiotemporal structure, representing local pulsations of glow in the field of view of the instrument. Geographical distribution was analyzed and it was shown that events are mainly located in the area of equatorial boundary of auroral oval (more than half of events were registered on L-shells 4–6). Characteristic frequencies of pulsations of glow intensity are of the order of 1–10 Hz, and areas of pulsating glow are localized in the space with characteristic horizontal size of 10–15 km. A comparison with the THEMIS ground-based all-sky cameras was made. 11 joint observations were found and the presence of aurora lights at the time of TUS events registration was shown by ground-based cameras, although no obvious coincidences of pulsations were found.

**Keywords** Flickering aurora · Pulsating aurora · Orbital telescope

## 1 Introduction

Numerous ground-based observations demonstrate the existence of a fine spatial and temporal structure of auroras, also mentioned as a flickering or pulsating aurora. Pulsating auroras are quasi-periodic variations of intensity of aurora luminescence

---

P. A. Klimov (✉) · K. F. Sigaeva  
Skobeltsyn Institute of Nuclear Physics Lomonosov Moscow State University, 1(2), Leninskie gory, Moscow 119234, Russia

K. F. Sigaeva  
Faculty of Physics, Lomonosov Moscow State University, 1(2), Leninskie gory, Moscow 119234, Russia

caused by precipitation of energetic electrons. They occur mainly in the MLT sector from midnight to morning after expansion of the auroral oval and during the substorm recovery phase. They appear as irregular patches of luminosity with quasi-periodic (2–20 s or more) temporal fluctuations, which are often accompanied by rapid complex movements of their bright part, synchronized with changes in luminosity [1]. The characteristic position for this type of auroras is on the equatorial edge of the auroral oval, shorter periods of pulsations appear at lower latitudes [2].

Analysis of ground-based optical observations of the flickering aurora showed the following features of the spatiotemporal structure. The width of the flickering column is in the range of 1–12 km [3], the lifetime of the flickering column is 1–2 s [4]. The luminosity modulation amplitude is less than 10–20% of the background luminosity, and typical frequencies are 3–15 Hz [5].

Various types of pulsating aurora are distinguished by the spatial structure and intensity modulation: pure pulsations (fixed size and shape), expanding pulsations, streaming aurora, etc. [6]. Three categories of pulsating aurora were proposed based on the stability of patch shape and spatial extent: Amorphous Pulsating Aurora (APA), Patchy Pulsating Aurora (PPA) and Patchy Aurora (PA) [7].

New measurements of fast pulsations in the near-ultraviolet (NUV) wavelength range in the auroral and subauroral regions were conducted by the TUS detector onboard the Lomonosov satellite with a high sensitivity and temporal resolution (6.6 ms). In what follows we present some results of these new data.

## 2 The TUS Detector and Data Selection

The Lomonosov satellite was launched on April 26, 2016 into a polar sun-synchronous orbit with an altitude of 470–500 km and an inclination of 97.3°, which allowed observations in the polar region. The TUS detector consists of two main parts: a mirror-concentrator and a photodetector in its focal plane. The photodetector pixels are 256 Hamamatsu R1463 photomultiplier tubes (PMTs). Each pixel has a black hood that protects it from side illumination, as well as a UV filter (300–400 nm) with a diameter of 13 mm and a thickness of 2.5 mm. PMTs are arranged in the following way—256 pixels are grouped into 16 identical modules, having a common system of high-voltage power supply, system of data acquisition and primary processing. More details about the TUS telescope can be found in [8].

The electronics of the photo detector operate in four modes, designed to register transient atmospheric events with different temporal resolution. The main mode has a resolution of 0.8  $\mu$ s. It is designed to measure extensive air showers as well as fastest transient atmospheric events, such as elves. Other modes of the TUS detector have lower temporal resolution: 25.6  $\mu$ s and 0.4 ms for recording slower events, such as sprites and various jets, and 6.6 ms for recording the slowest events: micrometeors, space debris, and auroras, the latter are analyzed in this paper.

In this mode, the TUS detector operated for three small intervals of time: 26.12.2016–10.01.2017, 28.02.2017–21.03.2017, 08.11.2017–15.11.2017,

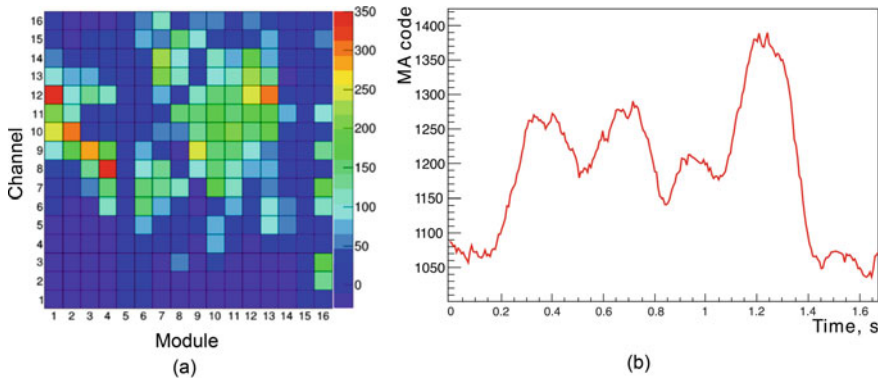


**Fig. 1** Example of the event with NUV pulsations measured by the TUS detector November, 10, 2017 at 13:31 UTC: Pixel map (a), waveform of one pixel: module 7, channel 12 (b)

and during this time about ten thousand events were registered, 2575 of them at high latitudes (more than  $50^\circ$ ) in the Northern Hemisphere. In the Southern Hemisphere at that time at the same latitudes was polar day, and registration of events was not conducted there.

Among all data several types of events were identified: (1) Stationary noise (majority of events where signal intensity fluctuates around a certain value). (2) Stationary source on the surface of the Earth or in the atmosphere: cities, clouds (maximum intensity of signal moves along the detector matrix at the speed of a satellite). (3) Thunderstorms and lightning discharges (events with sharp peaks of high intensity, which corresponds to lightning return strokes). (4) Events with unusual pulsations of the NUV signal at high latitudes.

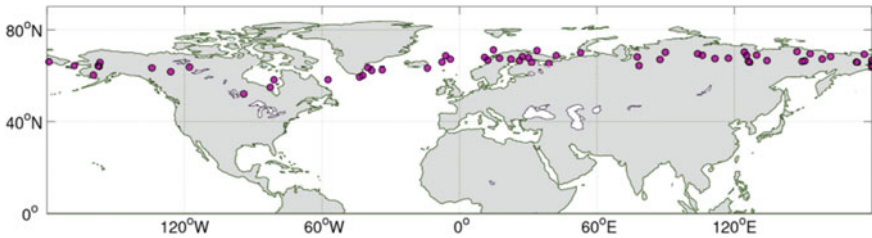
The first three types of events were excluded from the further analysis. And only 66 events of the last type were considered.

Figure 1a shows pixel map of one such pulsating event and demonstrates the spatial structure of the event. Figure 1b shows the waveform of a single pixel (module 7, channel 12). The signal growth is observed for 1.2 s with a pulsation. The pulsation period is about 0.3 s, and the amplitude is 10% of the background level. These temporal features are close to ones described in [5].

## 3 Results

### 3.1 Geographical Distribution and Geomagnetic Activity Analyses

The geographical location of the events is shown in Fig. 2. As can be seen, all events are located along the aurora region at latitudes from  $52$  to  $71^\circ$  N. The events were



**Fig. 2** Map of selected events with NUV pulsations (violet dots)

recorded both over the ocean and over land, which excludes the influence of the anthropogenic factor. The distribution of these events over the L-shell was studied. It appears that most of the events were measured when the satellite was between 4 and 6 L-shell, i.e. close to the equatorial edge of the auroral oval and even further south.

In this work, the AE-index was used to estimate the level of geomagnetic activity at the time of measuring the events. The AE-index data were provided by the World Data Center for Solar-Terrestrial Physics in Moscow (<http://www.wdcb.ru>). The majority of events is located during high geomagnetic activity during the substorm recovery phase. The example of AE-index behavior during the third period of measurements when a half of events were registered is shown at Fig. 3. All events are recorded at the local maxima of the AE index or at the stage of its decrease after the peak. Distribution of the number of NUV pulsation events by the AE-index is shown in Fig. 4a. It can be seen that the maximum number of events (33) was measured in the 200–400 nT interval. Comparison with the distribution of all events registered by the detector was also carried out to obtain the real frequency of occurrence of events in different periods of geomagnetic activity. The black histogram in the Fig. 4b shows the distribution of observation times by AE-index. And the green histogram shows

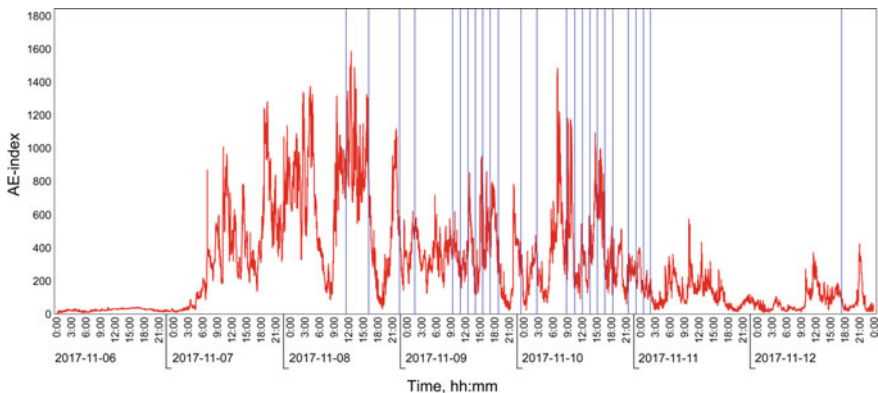


**Fig. 3** AE-index variations during the period of measurements 06.11.2017–12.11.2017. Blue lines indicate the TUS events

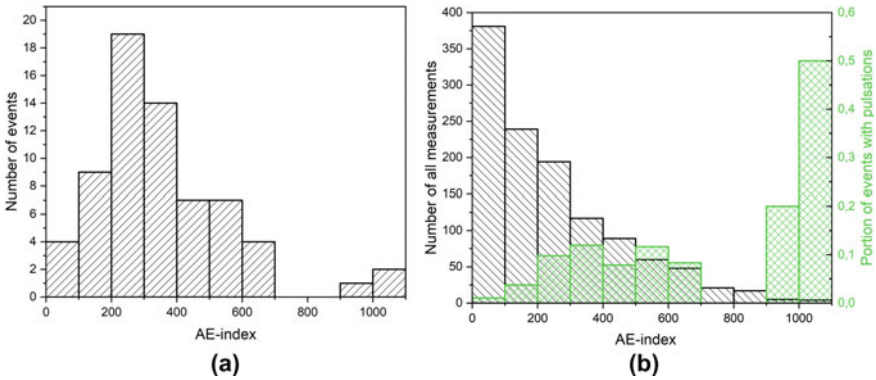


**Fig. 4** Distribution of events with NUV pulsations by AE-index (a). Distribution of all measurements at high latitudes by AE-index (black) and portion of events with pulsations (green) (b)

events frequency normalized by the observation time for a given AE-index. Thus, it is clearly seen that the effective fraction of events with pulsations during strong geomagnetic perturbations increases.

The distribution of events by MLT is shown in Fig. 5. It can be clearly seen that the most of NUV pulsation events were observed around MLT midnight, but is it mostly due to the satellite orbit parameters. The Lomonosov satellite had a sun-synchronous polar orbit and passed over aurora latitudes equator at a fixed local time around midnight.

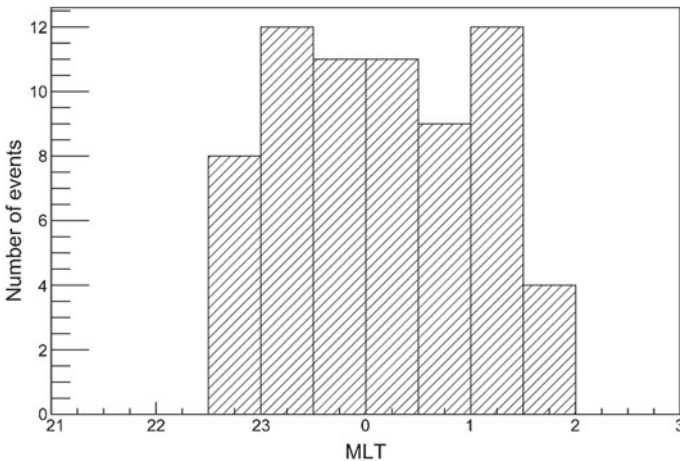


**Fig. 5** Distribution of events with NUV pulsations by MLT

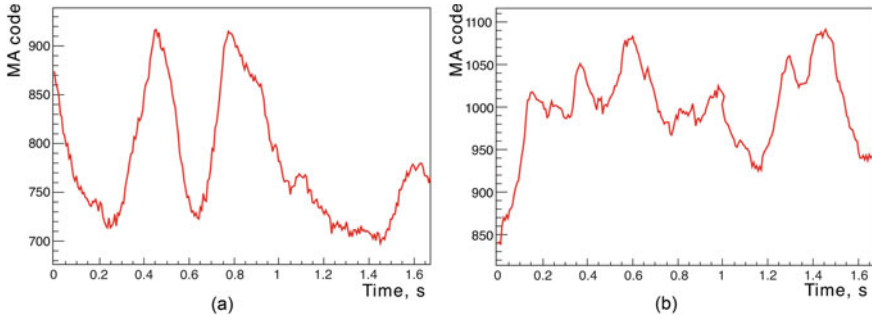


**Fig. 6** Waveforms of two pixels for two events. The event measured on 06.01.2017 at 05:18:26 UTC, demonstrates low frequency (2 Hz) repeating structures (a). The event measured on 06.01.2017 at 05:18:26 UTC with higher frequency pulsations ( $> 10$  Hz) (b)

### 3.2 Temporal and Spatial Structure of Events

The time structure of the registered events is quite diverse: different intensity, number of pulsations and their period. Examples of such events are shown in Fig. 1 and in Fig. 6. It is well seen from the figures that the frequencies of pulsations differ clearly. The study of frequency distribution demonstrates that most frequently measured pulsations lie in the region of 3 and 5 Hz, but there are events with frequencies up to 20 Hz.

The recorded events are characterized by the different temporal structures in different parts of the matrix. An example of the distribution of temporal structures over a part of the detector matrix is shown in Fig. 7. It demonstrates the oscillograms of 20 neighboring pixels. It can be seen that in the down left part of this matrix fragment only one slow peak is observed, while in the central part there are pulsations with 3 Hz modulation. There are three pixels with zero signal. These channels were broken. So, in the photo detector matrix various temporal structures can be seen simultaneously which means that spatially they occur in a part of the detectors FOV.

The FOV of one instrument pixel is 10 mrad, which corresponds to an area of  $5 \times 5$  km on the Earth's surface (and  $4 \times 4$  km at an altitude of 100 km). The observed structure changes from pixel to pixel in the recorded events suggest that the typical horizontal source size is about 10 km.

### 3.3 Comparison with THEMIS All-Sky Ground-Based Cameras Data

The data recorded by the TUS detector was compared with data from the THEMIS all-sky ground-based cameras [9]. This system of cameras is located so that it covers the entire sky over North America in the area of aurora observations. Temporal

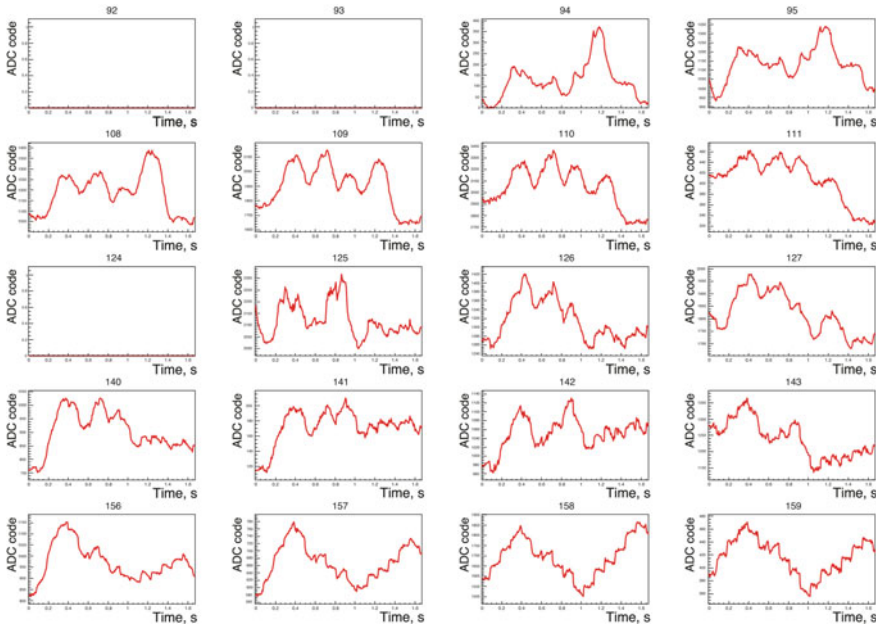


**Fig. 7** Waveforms of part of photodetector. Event measured on 10.11.2017 at 13:31 UTC above Chukotka. Three pixels with zero signal are inoperative

resolution is only 3 s, and thus it cannot measure fast pulsations, but its data allows one to understand the general activity and global structure of aurora emission.

A total of 11 data intersections were found (see Table 1) in measurements of the TUS detector and THEMIS camera array. Analysis of the joint observations of events showed that during the registration of events by the TUS detector active aurora luminescence was observed over North America.

One example of joint observations carried out on 06 January, 2017 at 05:17:33 UTC is presented in Fig. 8. On the panel **a** of the figure there is a map of images from all-sky THEMIS cameras. The red dot marks the place of event registration by the TUS detector. According to THEMIS cameras data the presence of auroras at the time of event registration is clearly visible (bright arc over the north of Canada). In the camera which corresponds to the TUS event only dim diffuse light is seen. It might be closed by clouds at the time of measurements or its sensitivity is not enough to register the same pulsations as TUS. On the panel **b** of the figure one of the oscillograms of the detector matrix at the moment of pulsations measurements is shown. Variations of luminescence at this moment are clearly seen on the oscillogram. The same situation is seen in Fig. 9: bright and variable aurora luminescence in the majority of THEMIS cameras. TUS events are on the edge of westernmost camera, but above the cloud coverage.

So, the TUS detector can provide an additional information of fine temporal structure of faint NUV emission in aurora due to its high aperture and sensitivity.

**Table 1** List of TUS events measured in the THEMIS all-sky cameras FOV

Date	Time UTC	Lat	Long	L	MLAT	MLT	Ae	THEMIS station code
2017-01-03	11:19:57	64.23	-168.06	4.46	61.68	23.17	614	KIAN
2017-11-10	10:24:54	60.17	-159.75	3.69	59.15	22.88	175	MCGR
2017-01-08	10:38:19	64.22	-157.69	4.90	63.30	23.09	555	KIAN
								MCGR
2017-11-10	10:23:52	63.97	-157.23	4.84	63.15	22.83	175	KIAN
								MCGR
2017-01-01	10:39:41	65.67	-156.91	5.50	64.78	23.09	286	KIAN
								MCGR
2017-11-10	08:49:54	63.30	-134.19	6.19	66.32	22.80	462	WHIT
2017-01-06	08:24:59	61.62	-126.00	6.15	66.06	23.12	220	FSIM
2017-01-07	07:57:16	63.64	-117.82	8.25	69.22	23.14	287	FSIM
								EKAT
2017-01-01	6:00:49	51.95	-94.16	4.40	60.52	23.45	285	GILL
								TPAS
2017-01-06	5:18:26	54.82	-82.57	5.32	64.05	23.63	266	SNKQ
2017-01-06	5:17:33	58.11	-80.95	6.73	67.40	23.72	265	SNKQ

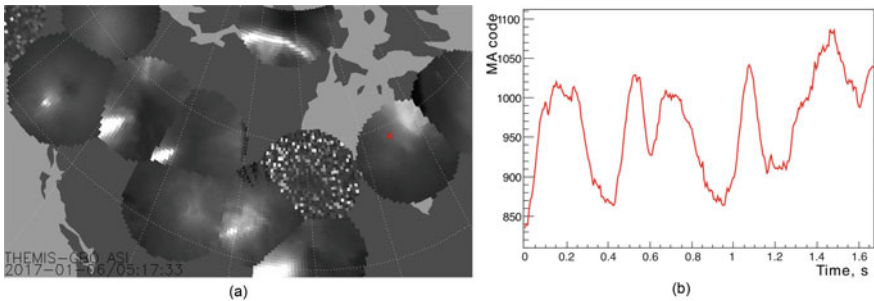


**Fig. 8** Map of images from THEMIS all-sky ground cameras, red dot shows the place of TUS detector at that moment (a). Waveform of one pixel for the event measured on 06.01.2017 at 05:17:33 UTC (b)

## 4 Conclusions

During the operation of the TUS detector on orbit NUV pulsations of atmospheric glow at high latitudes were registered. It became possible due to high sensitivity of the telescope, and the polar orbit of the spacecraft.



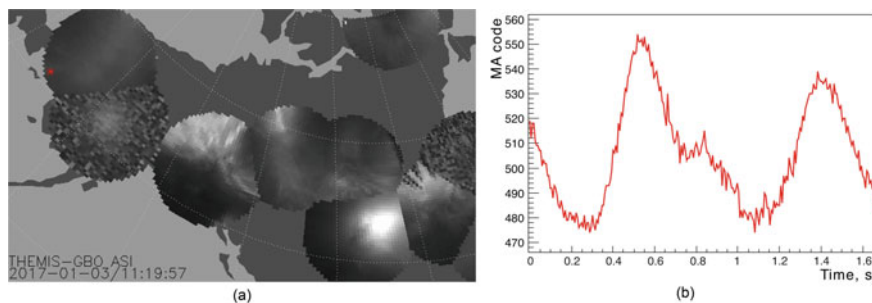


**Fig. 9** Map of images from THEMIS all-sky ground cameras, red dot shows the place of TUS detector at that moment (a). Waveform of one pixel for the event measured on 03.01.2017 at 11:19:57 UTC (b)

The structure of the recorded signals is quite diverse, but all the described events have the following characteristic features in common: frequencies of the order of 1–10 Hz and the spatial size of the pulsations about 10 km. In the FOV of the telescope we can simultaneously observe several different regions of pulsations with different temporal structures.

Analysis of geographical distribution and geomagnetic conditions showed that events were recorded at latitudes from 52 to 71° N. The location of these events does not depend on the level of geomagnetic activity. Most pulsations were registered at L-shells from 4 to 6, which corresponds to the equatorial edge of the auroral zone. However, the event's appearance frequency correlates with the geomagnetic activity.

A comparison was made between the TUS detector measurements and THEMIS all-sky ground-based camera data. The analysis showed the presence of bright polar lights at the time of registration of events in most cases. However, the pulsations themselves are not visible on the cameras, possibly because the TUS detector is much more sensitive than the cameras and recorded more faint emissions. Due to the TUS detector design, it can record events with even faster pulsations (such as those recorded in [10]), if sufficient exposure is achieved.

The spatial and temporal structure of the registered events is similar to the previously observed flickering auroras [5] and to the internal modulations of pulsating auroras associated with the high-energy part of the precipitating electrons caused by LBC waves. However, their nature and mechanism of occurrence are not yet clear. To study and clarify the nature of this phenomenon, further experiments on high-sensitivity orbital detectors, as well as the comparison of data obtained on satellites with data from ground-based observatories, are needed.

**Acknowledgements** The authors are grateful to the Lomonosov collaboration and the TUS detector development team. The work was done with partial financial support from the State Space Corporation ROSCOSMOS and the Interdisciplinary Scientific and Educational School of Moscow University "Fundamental and Applied Space Research".

## References

1. Yamamoto, T.: On the temporal fluctuations of pulsating auroral luminosity. *J. Geophys. Res.: Space Phys.* **93**, 897–911 (1988)
2. Duncan, C., Creutzberg, F., Gattinger, R., Harris, F., Jones, A.: Latitudinal and temporal characteristics of pulsating auroras. *Can. J. Phys.* **59**, 1063–1069 (2011). <https://doi.org/10.1139/p81-140>
3. Sakanoui, K., Fukunishi, H.: Temporal and spatial structures of flickering aurora derived from high-speed imaging photometer observations at Syowa station in the Antarctic. *J. Geophys. Res. Space Phys.* **109**, A01221 (2004). <https://doi.org/10.1029/2003JA010081>
4. Kunitake, M., Oguti, T.: Spatial-temporal characteristics of flickering spots in flickering auroras. *J. Geomagn. Geoelectr.* **36**, 121–138 (1984). <https://doi.org/10.5636/jgg.36.121>
5. Sakanoui, K., Fukunishi, H., Kasahara, Y.: A possible generation mechanism of temporal and spatial structures of flickering aurora. *J. Geophys. Res.* **110**, A03206 (2005). <https://doi.org/10.1029/2004JA010549>
6. Nishimura, Y., Lessard, M.R., Katoh, Y., Miyoshi, Y., Grono, E., Partamies, N., Sivasdas, N., Hosokawa, K., Fukizawa, M., Samara, M., Michell, R.G., Kataoka, R., Sakanoui, T., Whiter, D.K., Oyama, S.I., Ogawa, Y., Kurita, S.: Diffuse and pulsating aurora. *Space Sci. Rev.* **216**, 4 (2020). <https://doi.org/10.1007/s11214-019-0629-3>
7. Grono, E., Donovan, E.: Differentiating diffuse auroras based on phenomenology. *Ann. Geophys.* **36**, 891–898 (2018). <https://doi.org/10.5194/angeo-36-891-2018>
8. Klimov, P.A., Panasyuk, M.I., Khrenov, B.A., Garipov, G.K., Kalmykov, N.N., Petrov, V.L., Sharakin, S.A., Shirokov, A.V., Yashin, I.V., Zotov, M.Y., Biktemerova, S.V., Grinyuk, A.A., Grebenyuk, V.M., Lavrova, M.V., Tkachev, L.G., Tkachenko, A.V., Park, I.H., Lee, J., Jeong, S., Martinez, O., Salazar, H., Ponce, E., Saprykin, O.A., Botvinko, A.A., Senkovsky, A.N., Puchkov, A.E.: The TUS detector of extreme energy cosmic rays on board the Lomonosov satellite. *Space Sci. Rev.* **212**, 1687–1703 (2017). <https://doi.org/10.1007/s11214-017-0403-3>
9. Donovan, E., Mende, S., Jackel, B., Frey, H., Syrjäso, M., Voronkov, I., Trondsen, T., Peticolas, L., Angelopoulos, V., Harris, S., Greffen, M., Connors, M.: The THEMIS all-sky imaging array-system design and initial results from the prototype imager. *JASTP* **68**(13), 1472–1487 (2006). <https://doi.org/10.1016/j.jastp.2005.03.027>
10. Kataoka, R., Miyoshi, Y., Hampton, D., Ishii, T., Kozako, H.: Pulsating aurora beyond the ultra-low-frequency range. *J. Geophys. Res. (Space Phys.)* **117**, A08336 (2012). <https://doi.org/10.1029/2012JA017987>